JOURNAL OF COLLOID AND INTERFACE SCIENCE **206,** 66–76 (1998)
ARTICLE NO. CS985708

A Study of the Aggregation Behavior of Hexyltrimethylammonium Bromide in Aqueous Solution

Victor Mosquera,* José Manuel del Río,*,[1] David Attwood,† Manuel García,* Malcolm N. Jones,‡ Gerardo Prieto,* María José Suarez,* and Félix Sarmiento*,[2]

**Grupo de Física de Coloides y Polímeros, Departamento de Física Aplicada y Departamento de Física de la Materia Condensada, Facultad de Física, Universidad de Santiago de Compostela, E-15706 Santiago de Compostela, Spain; †School of Pharmacy, University of Manchester, Manchester M13 9PL, United Kingdom; and ‡School of Biological Sciences, University of Manchester, Manchester M13 9PT, United Kingdom*

Received December 2, 1997; accepted June 19, 1998

The self-association of *n*-hexyltrimethylammonium bromide (C_6TAB) in aqueous solution has been examined as a function of temperature and electrolyte concentration. The critical micelle concentration (CMC) and the degree of counterion binding (β) were determined by conductivity measurement at temperatures over the range 288.15–318.15 K. Ultrasound velocity measurements were used to obtain the CMC in water and in a range of concentrations of electrolyte (0.1 to 0.6 mol kg^{-1} NaBr) and static light scattering to obtain the aggregation number and the degree of counterion binding in water at 298.15 K. The enthalpy change on micellization in water was measured by microcalorimetry. Apparent adiabatic compressibilities were calculated from a combination of density and ultrasound velocity measurements. Changes in the thermodynamic properties on micellization were determined by applying the mass action model; good agreement was found between experimental and theoretical enthalpy changes. From comparison with the properties of other *n*-alkyltrimethylammonium bromides it has been shown that the CMC of C_6TAB in water is lower than that predicted from the linear relationships between CMC and the number of carbon atoms in the alkyl chain. Similarly, the standard Gibbs energy of micellization is less negative than predicted, and the degree of counterion binding is much lower than for other C_nTABs. It is suggested that the anomalous behavior of C_6TAB is a consequence of the more highly organized core of the aggregates of very low aggregation number (3–4) and the high degree of exposure of the micellar components to the aqueous environment.

Key Words: **hexyltrimethylammonium bromide; critical micelle concentration; micelles; adiabatic compressibility; thermodynamics of micellization.**

INTRODUCTION

Surfactant molecules self-associate in aqueous solution because the reduction of the hydrocarbon–water interface is energetically favored; the critical concentration at which aggregation occurs reflects the balance between the hydrophobic interaction of the hydrocarbon parts of surfactant molecules and the hydration and electrostatic repulsive effects of hydrophilic head groups (1). Both the critical micelle concentration (CMC) and the properties of aggregates are governed by several factors including the affinity and size of the counterion, size of the head group, length of the hydrocarbon chain, ionic strength, and pH (2).

Several authors have reported systematic studies on the micellar behavior of the *n*-alkyltrimethylammonium bromide series (C_nTAB). Zielinski *et al.* (3, 4) reported on the adiabatic compressibilities and apparent molar volumes of octyl-, decyl-, dodecyl-, and tetradecyltrimethylammonium bromides. De Lisi *et al.* (5) measured the thermodynamic properties of nonyl- and decyltrimethylammonium bromides. Micellar size has been determined by both static and dynamic light scattering techniques (6–9), and the transformation of shape of aqueous micelles of the C_nTAB series from spherical to ellipsoidal with increase of hydrocarbon chain length from 8 to 16 has been discussed by several authors (10–12). Zana (13) reported on the ionization of micelles of the alkyltrimethylammonium bromides with alkyl chain lengths from 8 to 16. In previous publications (14–16), we investigated the micellar behavior of C_nTAB with n = 8, 10, 12, and 14 in different media and at several temperatures to gain information on the effect of pH and alkyl chain length on the thermodynamics of micellization of these surfactants. In this study, we have extended the work on the C_nTAB series by a detailed examination of the physicochemical properties of aqueous solutions of C_6TAB. Preliminary evidence suggesting the possibility of self-association of this surfactant was from the apparent solubilization of the water-insoluble dye Sudan IV by concentrated aqueous solutions of C_6TAB. As far as we are aware, the aggregation characteristics of this surfactant have not previously been reported.

EXPERIMENTAL

Materials

n-Hexyltrimethylammonium bromide (C_6TAB) and *n*-hexadecyltrimethylammonium bromide (Lancaster MTM Research

[1] Present address: Facultad de Ciencias, Universidad Autónoma del Estado de México, 50000 Toluca, Estado de México, Mexico.

[2] To whom correspondence should be addressed. E-mail: faiacm@uscmail.es.

0021-9797/98 $25.00

Chemicals Ltd.) had purities >98% and were used without further purification. Water was doubly distilled, deionized, and degased before use. Sodium bromide was AnalaR grade.

Conductivity Measurements

The conductance was measured by using a conductivity meter (Kyoto Electronic type C-117), the cell of which was calibrated with KCl solutions in the appropriate concentration range. The cell constant was calculated using molar conductivity data for KCl published by Shedlovsky (17) and Chambers *et al.* (18). C_6TAB solutions of known molal concentration were progressively added to water using an automatic pump (Dosimat 665 Metrohm). The measuring cell was immersed in a thermostat bath, maintaining the temperature constant to within ±0.01 K. Temperature control was achieved using a Hewlett Packard vectra computer.

Density Measurements

Density was measured at 298.15 K using a Anton Paar 60/602 densimeter with a resolution of 10^{-6} g cm^{-3}. Temperature control was maintained within ±0.005 K giving rise to uncertainties in density of ca. ± 1.5×10^{-6} g cm^{-3}.

Ultrasound Velocity Measurements

Ultrasound velocity was measured at 298.15 K at a frequency of 2 MHz using a Nusonic model 6380 concentration analyzer (Nusonic, Inc.) with a temperature transducer connected to a Hewlett-Packard digital microvoltimeter 3455A. The sound velocity transducer was connected to a Hewlett-Packard multimeter 3437A, the output of which was accessed continuously by a computer giving an accuracy in the velocity of ±0.01 m s^{-1}. Temperature control was ±0.005 K, giving rise to uncertainties in the measurement of ultrasound velocity of ca. ± 0.05 m s^{-1} at molalities above the critical concentration. Measurements on more dilute solutions were subject to increased error associated with the adsorption of C_6TAB from solution onto the walls of the cell.

Static Light-Scattering Measurements

Static light-scattering measurements were made with a Malvern PCS 100 light-scattering instrument with vertically polarized light of wavelength 488 nm supplied by a 2-W argon ion laser (Coherent Innova 90). Solutions were clarified by ultrafiltration through 0.1-μm filters until the ratio of light scattering at angles of 45° and 135° did not exceed 1.10. The refractive index increment of the aggregates of C_6TAB was measured using an Abbé 60/ED precision refractometer (Bellingham and Stanley Ltd.).

Calorimetric Measurements

The calorimetric measurements were performed at 298.15 K with a Beckman 190B microcalorimeter. This is a twin differential calorimeter in which the heat produced in the reaction vessels is rapidly conducted through two surrounding thermopiles to an aluminum heat sink in which they are encased. The thermopiles surrounding each reaction vessel are wired in opposition in order that the thermoelectric response is a measure of the difference in heat flux from the two vessels. The entire system is held in position by a yoke which can be rotated to mix the components in the reaction vessels, heat effects due to the rotation and friction in each vessel cancelling. The calorimeter was calibrated as described by Pilcher *et al.* (19). The reaction vessel was charged with 1 g of solution of known molality and 1 g of water; the reference vessel contained 2 g of water. Hence, on mixing the final molality was reduced to half of its original value.

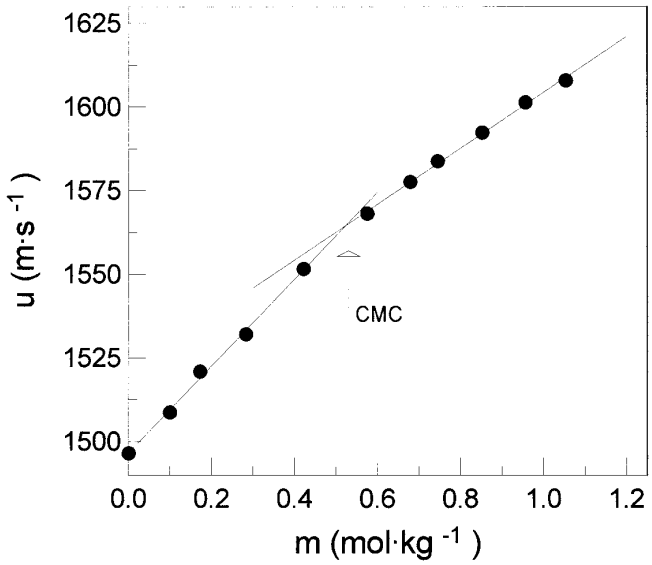

FIG. 1. Ultrasound velocity u of *n*-hexyltrimethylammonium bromide in water as a function of molality at 298.15 K. The arrow denotes the CMC.

RESULTS

Critical Micelle Concentration and Counterion Binding

The influence of electrolyte on the CMC was investigated using the ultrasound velocity technique. A plot of ultrasound velocity u, as a function of total C_6TAB molality m over a wide concentration range at a temperature of 298.15 K is illustrated in Fig. 1. The two linear segments of the plot, corresponding to the monomeric and micellar forms of the surfactant, intersect at the CMC. Similar plots were obtained for C_6TAB in the presence of NaBr from which the CMC values of Table 1 were derived. To obtain the degree of counterion binding β, the data of Table 1 were plotted according to

$$\log \text{CMC} = -\beta \log X^- + \Delta G_m^o/2.303RT + (1/n)\log F(M^{+p}) \quad [1]$$

TABLE 1

Critical Micelle Concentrations (CMC) Obtained from Ultrasound Velocity Measurements of *n*-Hexyltrimethylammonium Bromide as a Function of NaBr Concentration at 298.15 K

NaBr (mol kg^{-1})	CMC (mol kg^{-1})
0.0	0.495
0.1	0.347
0.3	0.320
0.4	0.290
0.5	0.285
0.6	0.250

where M^{+p} is the mole fraction of micelles at the CMC, n is the aggregation number, X^- is the counterion concentration, and F is a term involving activity coefficients for all species in solution (20). The degree of counterion binding determined from the gradient of the plot for C_6TAB was 0.3. The value of the standard free energy of micellization, ΔG^o_m, calculated from the intercept of the plot was -12.40 kJ mol^{-1}. This value is approximate as it was necessary to disregard the final term of Eq. [1] in the calculation of ΔG^o_m because of a lack of information on the fraction of surfactant in micellar form at the CMC. The error associated with this approximation is likely to be greater than usual in view of the very low aggregation number involved (see following discussion).

The influence of temperature on the CMC was investigated using conductimetric methods. In Fig. 2 we show representative conductivity plots of molar conductivity Λ as a function of square root of molal concentration. Similar plots were obtained at temperatures over the range 288.15–318.15 K. CMC values determined from inflections in such plots are given in Table 2. The increase in slope of the plots of molar conductivity versus root concentration above the CMC is unusual. Generally the slope of such plots decreases above the CMC because the influence of electrical force relative to frictional force on the micelles is reduced as a result of counterion binding. In the absence of counterion binding, the electrical force increases with micelle aggregation number, whereas the frictional force increases only with the cube root of the aggregation number so, if it were not for bound counterions, the slope would increase above the CMC. However, for small micelles, these simple relationships probably do not hold.

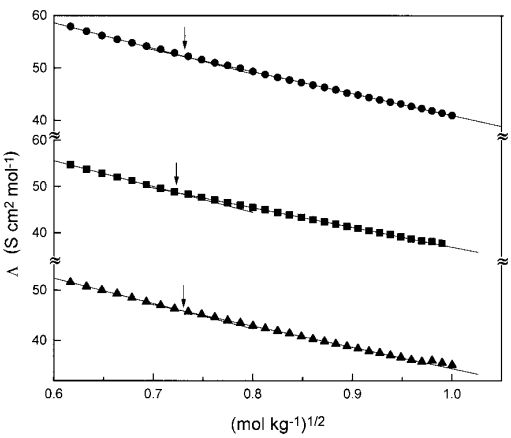

FIG. 2. Molar conductivity Λ of *n*-hexyltrimethylammonium bromide in water as a function of $m^{1/2}$ at (▲) 288.15 K, (■) 298.15 K, and (●) 318.15 K. The arrows denote the CMCs.

TABLE 2

Critical Micelle Concentrations (by Conductivity) and Standard Free Energy (ΔG^o_m), Enthalpy (ΔH^o_m), and Entropy (ΔS^o_m) of Micelle Formation per Mole of Monomer for *n*-Hexyltrimethylammonium Bromides in Water as a Function of Temperature

T (K)	CMC (mol kg^{-1})	ΔG^o_m (kJ mol^{-1})	ΔH^o_m (kJ mol^{-1})	ΔS^o_m (J K^{-1} mol^{-1})
288.15	0.535	−7.6	1.9	33
293.15	0.528	−7.8	1.2	31
298.15	0.524	−7.9	0.5	28
303.15	0.522	−8.1	−0.2	26
308.15	0.524	−8.2	−1.0	23
313.15	0.528	−8.3	−1.9	20
318.15	0.535	−8.4	−2.8	18

The variation of CMC with temperature can be described by the second-order polynomial

$$\text{CMC} = A_1 + A_2T + A_3T^2 \qquad [2]$$

with the coefficients $A_1 = 5.75 \pm 0.02$ mol kg^{-1}, $A_2 = -3.45 \times 10^{-2} \pm 1 \times 10^{-4}$ mol kg^{-1} K^{-1}, and $A_3 = 5.70 \times 10^{-5} \pm 2 \times 10^{-7}$ mol kg^{-1} K^{-2}. The minimum CMC value was at $T^* = 302 \pm 1$ K.

An approximate value of the degree of counterion binding β was calculated from the relationship

$$\beta = 1 - \alpha = 1 - S_2/S_1 \qquad [3]$$

with α being the degree of ionization, which was determined from the ratio of the mean gradients of conductivity against concentration plots above (S_2) and below (S_1) the CMC (21). A mean value of 0.3 was obtained; it was independent of temperature over the temperature range of the study. This value should be considered as an approximate value, not only because of the simplifications involved in the derivation of Eq. [3] but also in view of the contribution to the conductivity arising from the very small ionic micelles of this study.

Limiting molar conductivities at infinite dilution Λ_0 were derived by fitting the conductivity data to the Onsager equation in the form

$$\Lambda = \Lambda_0 - (A\Lambda_0 + B)m^{1/2}. \qquad [4]$$

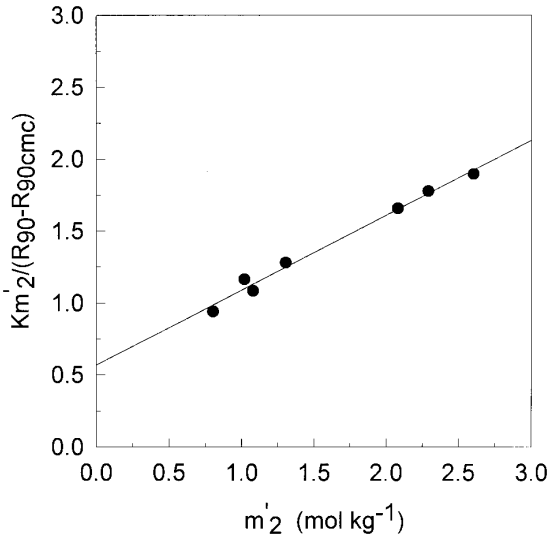

FIG. 3. Scattering function $Km_2'/(R_{90} - R_{90CMC})$ for *n*-hexyltrimethylammonium bromide in water as a function of micellar molality m_2' at 298.15 K.

Values of Λ_0 thus obtained (in S cm^2 mol^{-1}) were 94.7 ± 0.4 at 318.15 K, 94.0 ± 0.4 at 313.15 K, 90.1 ± 0.6 at 308.15 K, 89.2 ± 0.3 at 303.15 K, 83.9 ± 0.3 at 298.15 K, and 83.6 ± 0.7 at 288.15 K.

Micelle Size

The static light-scattering data are presented in Fig. 3 as plots of the scattering function $Km_2'/(R_{90} - R_{90CMC})$ against m_2', where R_{90} and R_{90CMC} are the Rayleigh ratios at 90° from a solution of molality m and a solution at the CMC, respectively; m_2' is m-CMC, and K is the usual optical constant for vertically polarized light. The scattering data were analyzed by the method proposed by Anacker and Westwell (22) which indicated an aggregation number (n) of the order of 3 and a degree of counterion binding of about 0.3, the latter being in agreement with the value from conductivity methods.

Thermodynamics of Micellization

Figure 4 shows the experimentally measured enthalpies of dilution ΔH of C_6TAB in water at a temperature of 298.15 K as a function of the final concentration. Three concentration zones may be observed. For $m < 0.4$ mol kg^{-1}, ΔH has a constant value of -1.52 ± 0.02 kJ mol^{-1}; for $0.4 < m < 0.7$ mol kg^{-1}, a transition zone exists in which the enthalpy is concentration-dependent suggesting that aggregates start to form; and for $m > 0.7$ mol kg^{-1}, ΔH again becomes constant, indicating well-defined aggregates. The broad width of the transition zone (approximately 0.3 mol kg^{-1}) is expected for micelles of low aggregation number. The enthalpy of micellization, calculated from the difference between values for the monomeric and micellar states (23) is 0.57 ± 0.02 kJ mol^{-1}.

The thermodynamic properties of micellisation were derived by application of the mass action model as follows. The equilibrium constant K_m for the formation of micelles may be written (24, 25)

$$\frac{1}{K_m} = n\,\frac{(2n-z)(4n-2z-1)}{2n-z-2} \times \left[\frac{(2n-z)(4n-2z-1)}{(2n-z-1)(4n-2z+2)}\,X_{CMC}\right]^{2n-z-1}, \quad [5]$$

where z is the net charge of the micelle ($z = n\alpha$) and X_{CMC} is the CMC as a mole fraction. In the calculation of K_m, values of $n = 3$ (light scattering) and $\alpha = 0.7$ (light scattering and conductivity) were used; both were assumed to be constant with temperature.

The variation of ln K_m with temperature T was attributed only to the temperature coefficient of the CMC and was fitted to a second-order polynomial of the form

$$\ln K_m = fT^2 + gT + h, \quad [6]$$

where $f = 0.03 \times 10^{-4} \pm 10^{-6}$ K^{-2}, $g = 0.1817 \pm 8 \times 10^{-4}$ K^{-1}, and $h = -18.0 \pm 0.1$. The plot of ln K_m against T is shown in Fig. 5.

Values (per mole of monomer) of the standard Gibbs energy change ΔG_m^o, the standard enthalpy change ΔH_m^o, and the standard entropy change ΔS_m^o, on micellization (see Table 2) were calculated from

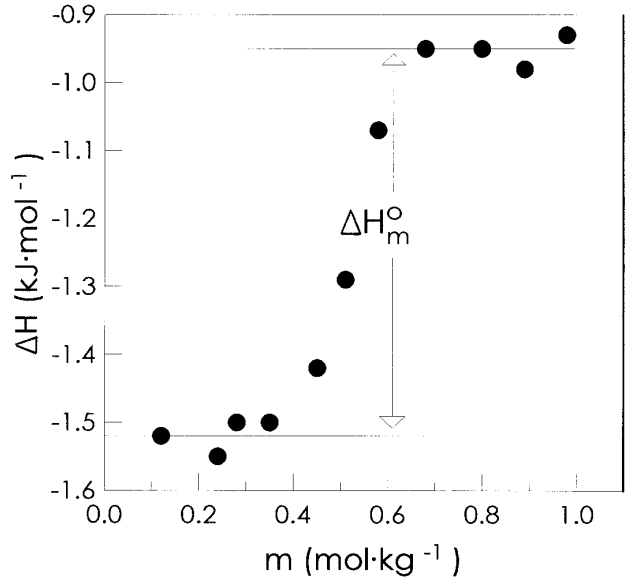

FIG. 4. Enthalpies of dilution (from $2m$ to m) ΔH of *n*-hexyltrimethylammonium bromide in water as a function of the final molality at 298.15 K.

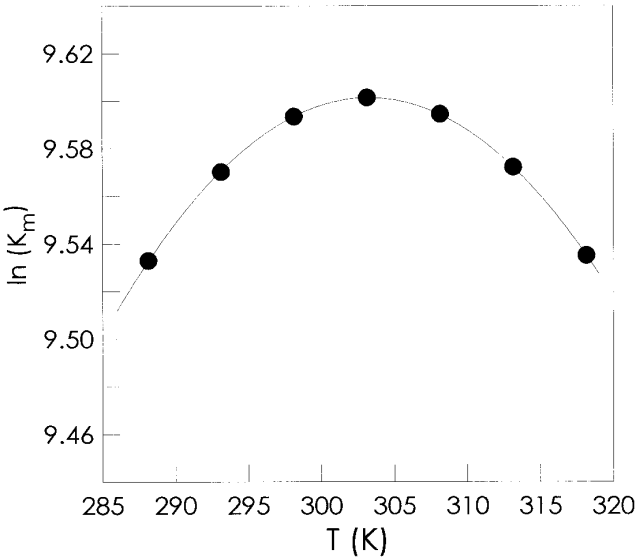

FIG. 5. Natural log of micellization equilibrium constant K_m of *n*-hexyltrimethylammonium bromide in water as a function of temperature. The continuous line is calculated from Eq. [6].

$$\Delta G^o_m = -(RT/n)\ln K_m, \quad [7]$$

$$\Delta H^o_m = \left[\frac{\partial(\Delta G^o_m)/T}{\partial\left(\frac{1}{T}\right)}\right]_P = \frac{RT^2}{n}\left(\frac{\partial \ln K_m}{\partial T}\right)_P, \quad [8]$$

$$\Delta S^o_m = -\frac{1}{T}(\Delta G^o_m - \Delta H^o_m). \quad [9]$$

The enthalpy change calculated at 298.15 K for $n = 3$ and $\beta = 0.3$ was 0.5 ± 0.2 kJ mol^{-1}, which compares with the experimental value of 0.57 ± 0.02 kJ mol^{-1} from microcalorimetry. The agreement between the van't Hoff and calorimetric enthalpies either suggests that micellization is highly cooperative or is fortuitous as a result of the neglect of activity coefficients in the estimation of K_m. If the latter were true, micellization would probably be less cooperative than this agreement suggests.

The influence of the value assumed for the aggregation number on the calculated enthalpy change was examined using a range of assumed *n* values. The ΔH^o_m value calculated using $n = 4$ was 0.7 ± 0.2 kJ mol^{-1}; higher *n* values gave ΔH^o_m values in poor agreement with the experimental value. Hence, the aggregation number of C_6TAB, which gives good agreement between the mass action enthalpy and the calorimetric value, is of similar magnitude to that from static light scattering.

Apparent Molar Volumes

Figure 6 compares the concentration dependence of the density ρ for aqueous solutions of C_6TAB and C_{16}TAB. Apparent molar volumes, ϕ_v were calculated from the density values using

$$\phi_v = \frac{M}{\rho} - \frac{10^3(\rho - \rho_o)}{m\rho\rho_o}, \quad [10]$$

where M is the molecular weight of the surfactant and ρ_0 is the density of pure water (0.997043 g cm^{-3} at 298.15 K). Figure 7 shows the ϕ_v values for C_6TAB and C_{16}TAB solutions as a function of $m^{1/2}$. The behavior of C_{16}TAB is characteristic of a typical surfactant showing an increase of ϕ_v with concentration above the CMC ($\cong$1 mmol kg^{-1}) as a result of the decreasing hydrophobic hydration or disruption of the hydration shell around the hydrocarbon moiety. In contrast, the apparent molar volume of C_6TAB decreases with a concentration increase above the CMC. This apparent volume contraction may be a consequence of the effects of electrostriction of the ionic groups and hydration of both ionic groups and hydrocarbon moiety (26).

In the concentration region $m \leq$ CMC, the apparent molar volume ϕ_1 for a 1:1 electrolyte may be described by

$$\phi_1 = \phi^o_1 + A_v m^{1/2} + B_v m, \quad [11]$$

where A_v is the Debye–Hückel limiting law coefficient (1.865 cm^3 kg$^{1/2}$ mol$^{-3/2}$ for a 1:1 electrolyte at 298.15 K). B_v is an adjustable parameter which measures the deviations from the limiting law, and ϕ^0_1 is the apparent molar volume at infinite dilution. The values determined by application of Eq. [11] to the experimental data for C_6TAB in the preCMC region were $\phi^0_1 = 193.82 \pm 0.05$ cm^3 mol^{-1}, $A_v = 1.8 \pm 0.2$ cm^3 kg$^{1/2}$ mol$^{-3/2}$, and $B_v = -3.4 \pm 0.2$ cm^3 kg mol^{-2}. As seen from Fig. 7, the gradient of such plots approaches zero at high surfactant concentration, and many workers have subjectively

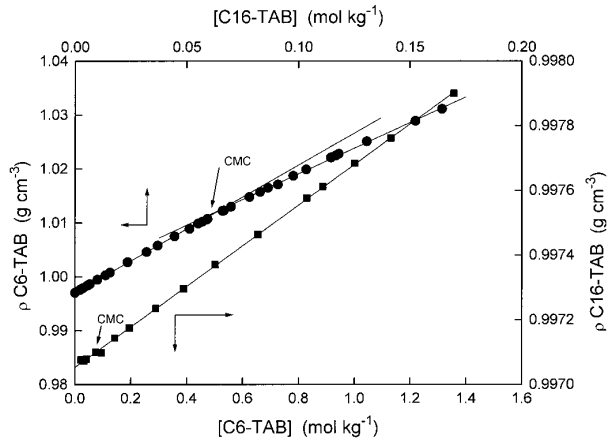

FIG. 6. Densities of *n*-hexyl and *n*-hexadecyltrimethylammonium bromides at 298.15 K as a function of the molality. (●) *n*-hexyltrimethylammonium bromide and (■) *n*-hexadecyltrimethylammonium bromide. The arrows denote the CMCs.

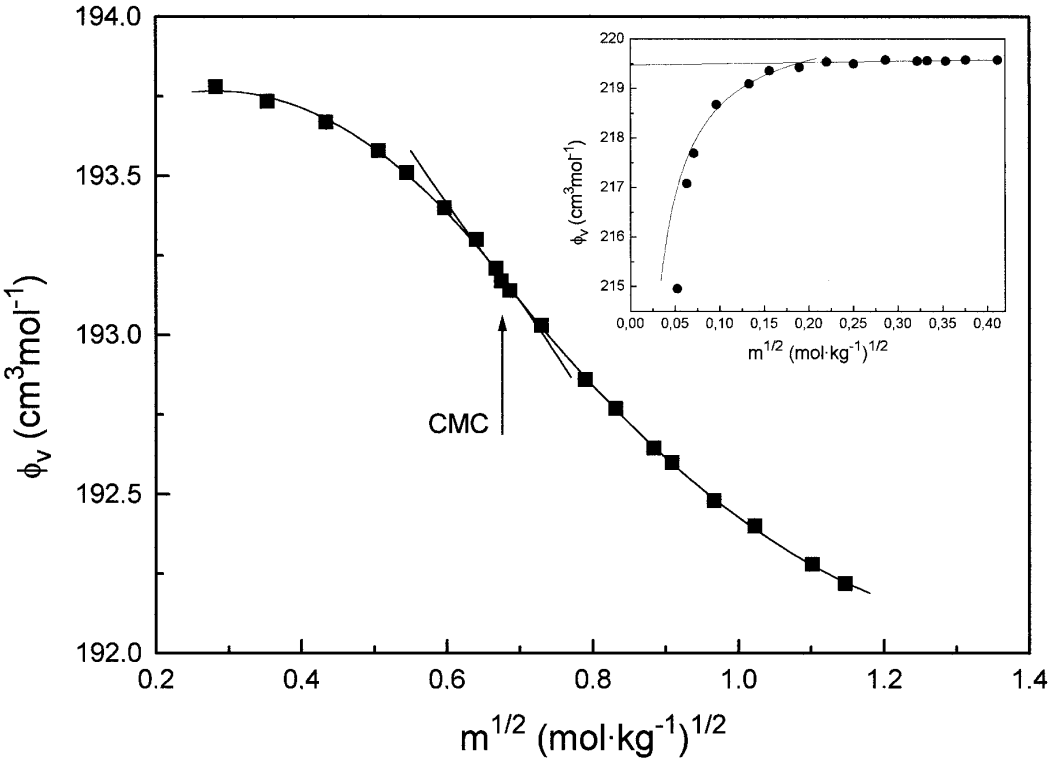

FIG. 7. Apparent molar volume ϕ_v of (■) *n*-hexyltrimethylammonium bromide and (●) *n*-hexadecyltrimethylammonium bromide in water at 298.15 K, as a function of square root of molality. The arrow denotes the CMC of *n*-hexyltrimethylammonium bromide.

chosen the approximately constant or limiting values as the apparent molar volume of the micelles ϕ_2. An alternative approach (27) is to fit these data to the function

$$\phi_v/\phi_2 = m/(a + m) \qquad [12]$$

where a is an empirical constant. Rearrangement to

$$\phi_v = -a(\phi_v/m) + \phi_2 \qquad [13]$$

enables ϕ_2 to be derived from plots of ϕ_v against ϕ_v/m. The value of ϕ_2 obtained in this way was 191.79 ± 0.03 cm^3 mol^{-1}. Thus, the change in volume associated with the formation of the stable aggregate from monomeric surfactant was taken to be $\Delta V_m = \phi_2 - \phi_1^0 = -2.03$ cm^3 mol^{-1}, which compares with an approximate value of -1.82 cm^{-3} mol determined from Fig. 7 by visual inspection.

Apparent Adiabatic Compressibility

Density and ultrasound velocity measurements were combined to calculate adiabatic compressibility k_s of C_6TAB solutions at 298.15 K using the Laplace equation

$$k_S = \frac{1}{\rho u^2}. \qquad [14]$$

The plot of k_s against concentration (Fig. 8) shows two linear segments with the intersection at the CMC. The linear regions may be assigned to monomeric and micellar forms, and values for the apparent adiabatic compressibilities of these

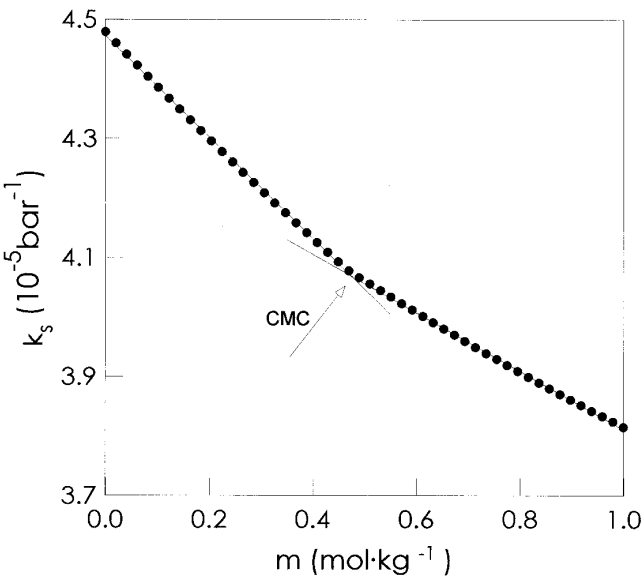

FIG. 8. Adiabatic compressibility k_S of *n*-hexyltrimethylammonium bromide in water at 298.15 K as a function of molality. The arrow denotes the CMC.

species may be calculated from the gradients of the relevant portions of the plot using

$$k_S = k_{S,0} + (\tilde{k}_{S,1} - k_{S,0})\tilde{\nu}_1 c_1 + (\tilde{k}_{S,2} - k_{S,0})\tilde{\nu}_2 c_2, \quad [15]$$

where $k_{s,0}$ is the adiabatic compressibility of the solvent, $\tilde{\nu}_1$ and $\tilde{\nu}_2$ are the apparent specific volumes of monomer and micelle, c_1 and c_2 are the monomer and micelle concentrations (in g cm^3), and $\tilde{k}_{S,1}$ and $\tilde{k}_{S,2}$ are the apparent adiabatic compressibilities of the monomeric and micellar species, defined as

$$\tilde{k}_{S,1} = -\frac{1}{\tilde{\nu}_1}\left(\frac{\partial \tilde{\nu}_1}{\partial p}\right)_S \quad [16]$$

and

$$\tilde{k}_{S,2} = -\frac{1}{\tilde{\nu}_2}\left(\frac{\partial \tilde{\nu}_2}{\partial p}\right)_S. \quad [17]$$

Values of the apparent specific volumes of monomers $\tilde{\nu}_1$ and micelles $\tilde{\nu}_2$ required for the calculation of the adiabatic compressibilities were determined from the gradients of linear portions of plots of density against concentration (Fig. 6) below and above the CMC using

$$\rho = \rho_0 + (1 - \tilde{\nu}_1\rho_0)c_1 + (1 - \tilde{\nu}_2\rho_0)c_2 \quad [18]$$

Values of $\tilde{k}_{S,1} = -0.12$ bar^{-1} and $\tilde{k}_{S,2} = 2.1$ bar^{-1} were obtained for C_6TAB and $\tilde{k}_{S,2} = 4.46$ bar^{-1} for C_{16}TAB at 298.15 K by this procedure.

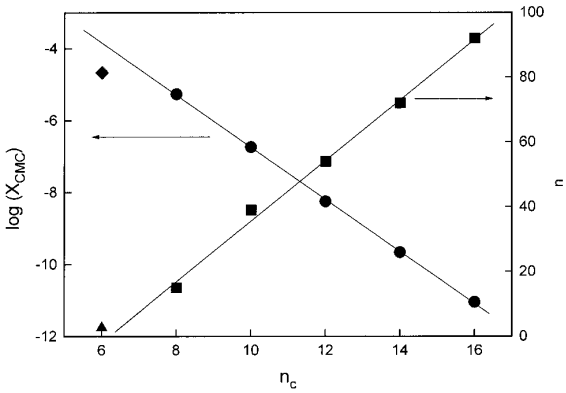

FIG. 9. Log of CMC (in mole fractions), $\log_{10} X_{CMC}$, and aggregation number n of n-alkyltrimethylammonium bromides in water at 298.15 K as a function of the hydrocarbon chain length. (●) Average CMC values from data of Table 3, (◆) CMC value from this work, (■) n values from Refs. 9 (C_8TAB) and 41 (C_{10} to C_{16}TAB), and (▲) n value from this work.

TABLE 3
Average CMC for n-Alkyltrimethylammonium Bromides in Water at 298.15 K

C_nTAB	CMC (mol dm^{-3})	References
C_6TAB	5.09×10^{-1}[a]	This work
C_8TAB	2.9×10^{-1}	(4, 9, 28, 29)
C_{10}TAB	6.61×10^{-2}	(4, 5, 24, 29–32)
C_{12}TAB	1.46×10^{-2}	(4, 24, 30, 31)
C_{14}TAB	3.54×10^{-3}	(4, 24, 28, 31, 33)
C_{16}TAB	8.9×10^{-4}	(4, 30, 31)

[a] Critical micelle concentration in mol kg^{-1} of water.

DISCUSSION

It is clear from the results obtained from this study that the aggregates present in aqueous solutions of hexyltrimethylammonium bromide are very small; our light-scattering measurements have indicated aggregates of aggregation number on the order of 3–4. Comparison with literature values (Fig. 9) shows that aggregates of this size would be expected if the linear decrease of n with n_c were continued to C_6TAB. Their small size calls into question whether these are true micelles in the accepted sense. Nevertheless, we have treated them as if they were micelles, and to a large degree they behave accordingly. However, in such small aggregates removal of the alkyl chains from the aqueous environment is not as effective as in the longer chain C_nTABs, and this may account for some deviation of the micellar properties from predicted values, as will be discussed.

Table 3 compares the CMC values of C_6TAB obtained at 298.15 K in this study with average literature values for other compounds of the C_nTAB series. In Fig. 9, we show $\log_{10}$ of the CMC (as a mole fraction) against the number of carbons n_c in the alkyl chain. This plot was fitted (C_6TAB values not included) to Eq. [2] such that

$$\log_{10} X_{CMC} = b_0 - b_1 n_c, \quad [19]$$

where $b_0 = 0.22 \pm 0.04$ and $b_1 = 0.315 \pm 0.003$, with a correlation coefficient of 0.998. It is clear that C_6TAB does not conform to Eq. [19] (i.e., the limit of applicability of this empirical expression for this homologous series is $8 \leq n_c \leq 16$).

Verral *et al.* (34) and Zana (13) found similar behavior when measuring the CMC for the series of dodecyldimethylalkylammonium bromides [$C_{12}H_{25}(C_mH_{2m+1})N(CH_3)_2Br$, $m = 1$ to 10] in aqueous solution as a function of chain length m. A deviation from linearity of plots of $\log_{10} X_{CMC}$ against m was observed at $m = 4$, which was attributed to a change in the location of the C_mH_{2m+1} chain from the micelle core ($m \geq 4$) to the micelle surface ($m \leq 3$). The deviation from linearity observed in the present study may be the result of exposure of

TABLE 4

Standard Free Energy (ΔG^{o}_{m}), Enthalpy (ΔH^{o}_{m}), and Entropy (ΔS^{o}_{m}) of Micellization and Degree of Counterion Binding (β) for *n*-Alkyltrimethylammonium Bromides in Aqueous Solution at 298.15 K. (References to literature values of β are given in parentheses.)

n_c	β	ΔG^{o}_{m} (kJ mol^{-1})[a]	ΔH^{o}_{m} (kJ mol^{-1})[b]	ΔS^{o}_{m} (J K^{-1} mol^{-1})
6	0.3	−7.9	0.5	28.2
8	0.65 (9)	−21.5	—	—
10	0.75 (31)	−29.2	0.2	98.6
12	0.79 (31)	−36.0	−2.3	112.7
14	0.82 (35)	−44.0	−4.9	131.5
16	0.89[c]	−51.7	−10.9[d]	136.8

[a] Calculated from CMC data (Table 3) and β values using Eq. [1].
[b] From microcalorimetry (36).
[c] Calculated from Ref. 31 using Eq. [1].
[d] Average value (36, 37).

the alkyl chains of the aggregates to the solvent as a consequence of their small size.

Table 4 shows much lower β values for C_6TAB in water at 298.15 K than expected from the literature values for other C_nTAB surfactants measured under the same conditions, which gradually decrease with decreasing chain length. A decrease of β (increase of α) is a consequence of a decrease of surface charge density (increase of surface area per ionic head group) (13). The large decrease of β noted in this study for a decrease of alkyl chain length from C_8 to C_6 is compatible with the large surface area per head group which would be associated with the micellar model proposed for this surfactant.

The standard thermodynamic quantities of micellization determined for C_6TAB are compared with those of other members of the C_nTAB series in Table 4. ΔG^{o}_{m} was calculated from the CMC data of Table 3, and the β values of Table 4 were calculated using Eq. [1]. With the exception of that of C_6TAB, the ΔG^{o}_{m} values conform ($r = 0.997$) to the empirical relationship

$$\Delta G^{o}_{m} = a_1 + a_0 n_c, \qquad [20]$$

where a_1 is a constant which depends on the temperature and the nature of the ionic head group and a_0 is interpreted as the CH_2 group contribution to the Gibbs standard free energy of micellization (1). A less negative ΔG^{o}_{m} associated with the micellization of C_6TAB compared with that predicted by Eq. [20] (−13.8 kJ mol^{-1}) may be a consequence of the ineffective removal of the hydrophobic groups from the aqueous environment in the small aggregates.

Figure 10 shows plots of ΔH^{o}_{m} and ΔS^{o}_{m} as a function of n_c. The literature values of the standard enthalpies of micelle formation ΔH^{o}_{m} (Table 4) have been determined by microcalorimetric techniques. The standard entropies of micellization ΔS^{o}_{m} were calculated from these values and the values of ΔG^{o}_{m} using Eq. [9]. Only a small variation of ΔH^{o}_{m} between $n_c = 6$ to 10 can be observed, whereas it changes sign, and its magnitude rapidly increases as n_c increases from 10 to 16. In contrast, ΔS^{o}_{m}, which is positive for all the chain lengths studied, increases rapidly from $n_c = 6$ to 10 and more slowly with increase of n_c for higher alkyl chain lengths. The plots of Fig. 10 show that the enthalpy change assists micellization at high n but opposes it at low n.

We may consider two contributions to the entropy change on micellization (23, 38). A restriction of movement of the hydrocarbon chains on transference to the interior of the micelle is associated with a negative entropy change ΔS_{HC}, whereas the loss of structured water during this transfer results in a positive entropy change ΔS_W. It is reasonable to assume that the magnitude of ΔS_W increases more or less linearly with an increase of chain length, and the nonlinear changes in ΔS^{o}_{m} observed in Fig. 10 arise mainly from the ΔS_{HC} contribution. The liquid state in the hydrocarbon core of a micellar assembly is appreciably different from the bulk liquid state. The hydrocarbon chains are unable to tumble, and, on average, remain oriented perpendicularly to the hydrocarbon–water interface. The influence of this surface anchoring becomes less significant the longer the chain because of an increase in the degree of freedom of chain movement; the longer the chain length, the more closely the micelle core resembles a quasi-liquid state (1). That is to say, the micellar core is more structured for low n_c values than for high values; hence, the ΔS_{HC} contribution may be expected to decrease with increase of the length of the alkyl chain. It is suggested from this reasoning that the large decrease of ΔS^{o}_{m} with decrease of n_c from 10 to 6 is the result of an anomalously high (negative) value of ΔS_{HC} at $n_c = 6$, from which we can deduce that the interior of the C_6TAB micelle is in a higher organization level than that of other surfactants of this homologous series.

A similar reasoning may be applied to explain the changes in ΔH^{o}_{m}. The transferance of alkyl chains from the aqueous environment to the liquid interior of the micelle is an exothermic

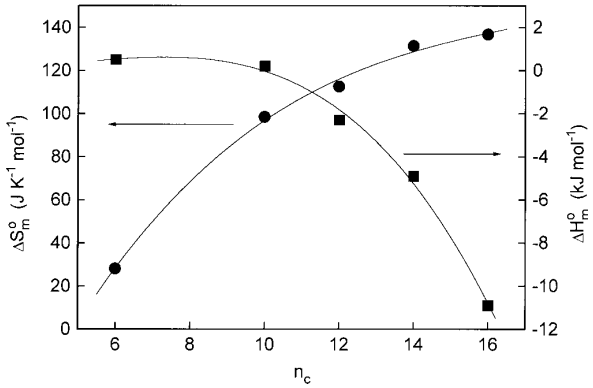

FIG. 10. (●) Standard entropy ΔS^{o}_{m} and (■) standard enthalpy ΔH^{o}_{m} of micellization at 298.15 K for *n*-alkyltrimethylammonium bromides as a function of alkyl chain length. Data are from Table 4.

process, whereas the loss of structured water during transfer (hydrophobic interaction) is endothermic (23). According to this reasoning, the positive ΔH_m^o from $n_c = 6$ to 10 is a consequence of a predominance of the hydrophobic interaction, and the increasingly negative ΔH_m^o value as n_c increases from 12 to 16 indicates the increasing importance of the London dispersion forces. This last conclusion is compatible with the explanation proposed for the changes in ΔS_m^o, providing the London dispersion force is the only interaction between the alkyl chains; the micelle core more closely resembling quasi-liquid state with the increase of alkyl chain length.

Figure 11 shows changes in the apparent molar volumes of the free monomer ($\phi_{v,1}$) and that of monomers in the micellar state ($\phi_{v,2}$) for the C_nTAB series. Both increase with the chain length, the free monomer molar volumes being smaller than those in the micellar state at the same chain length indicating that the monomer in the micelle is in a less-packed structure than the monomer in a free state. The difference between $\phi_{v,1}$ and $\phi_{v,2}$ becomes progressively smaller with the decrease of chain length, suggesting increasing constraints on molecular mobility as the micelle size decreases, which is in agreement with the explanation proposed above for changes in ΔS_m^o and ΔH_m^o. The increase of $\phi_{v,2}$ with the number of carbons fitted the linear equation $\phi_{v,2} = c_1 + c_0 n_c$, with $c_1 = 99 \pm 3$ cm^3 mol^{-1} and $c_0 = 16.4 \pm 0.2$ cm^3 mol^{-1} with a correlation coefficient of 0.9996. It is interesting to observe that the contribution of the CH_2 group obtained in this way (16.4 ± 0.2 cm^3 mol^{-1}) is very close to the one calculated from the atomic volumes, 16.1 cm^3 mol^{-1} (39, 40).

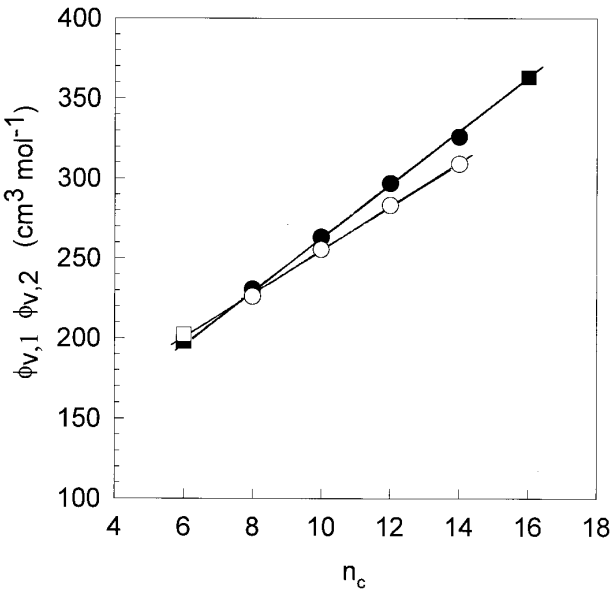

FIG. 11. Apparent molar volumes at 298.15 K of the *n*-alkyltrimethylammonium bromides in the monomeric form ($\phi_{v,1}$) and in the micellar state ($\phi_{v,2}$) of the *n*-alkyltrimethylammonium bromides as a function of the alkyl chain length. Symbols: (●) $\phi_{v,2}$ and (○) $\phi_{v,1}$ from Ref. 3. (■) $\phi_{v,2}$ and (□) $\phi_{v,1}$ from this work.

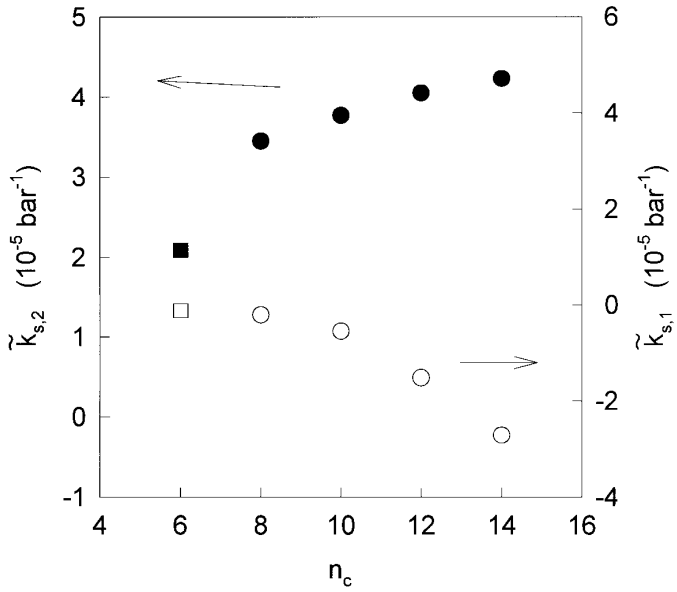

FIG. 12. Apparent adiabatic compressibilities at 298.15 K of *n*-alkyltrimethylammonium bromides in the monomeric form $\tilde{k}_{S,1}$ and in the micellar state $\tilde{k}_{S,2}$ as a function of the alkyl chain length. Symbols: (○) $\tilde{k}_{S,1}$ and (●) $\tilde{k}_{S,2}$ from Ref. 3. (□) $\tilde{k}_{S,1}$ and (■) $\tilde{k}_{S,2}$ from this work.

In Fig. 12, literature values of the apparent adiabatic compressibilities in monomeric $\tilde{k}_{S,1}$ and micellar $\tilde{k}_{S,2}$ forms are plotted as a function of the alkyl chain length for the C_nTAB series. Addition of the C_6TAB data to the available literature values shows that $\tilde{k}_{S,1}$ remains practically constant with increase of n_c to $n_c = 8$, whereas for higher values it decreases rapidly. Moreover, the apparent adiabatic compressibility of the micellar form $\tilde{k}_{S,2}$ is now seen to increase markedly between $n_c = 6$ and 8 and then more gradually with further increase of the length of the chain.

Changes in apparent adiabatic compressibilities may be explained by considering two types of hydration. The monomer in the micellar state has only hydrophilic (or ionic) hydration, whereas the monomer in a free state has both hydrophilic and hydrophobic hydration. The hydrophilic hydration occurs around the head group and involves interaction of hydrogen or oxygen atoms with the ionic group. The hydrophobic hydration is caused by the strong association of water molecules around the hydrophobe (iceberg structure). The $\tilde{k}_{S,1}$ value of C_6TAB is similar to that reported by Zielinski *et al.* (4) for C_1TAB, suggesting that its hydration is almost exclusively hydrophilic. The increase of hydrophobic hydration with alkyl chain length leads to the increasingly negative values of $\tilde{k}_{S,1}$ of Fig. 12 as n_c increases. The relatively small difference between $\tilde{k}_{S,1}$ and $\tilde{k}_{S,2}$ for C_6TAB suggests a high degree of hydration of monomers in the micelle. Zielinski *et al.* (4) attribute differences in the temperature dependence of $\tilde{k}_{S,2}$ of C_8TAB compared to C_nTABs of higher chain length to a penetration of water molecules to the interior of the micelle. C_8TAB micelles have an aggregation number of between 20 (9) and 23 (41) at 298.15

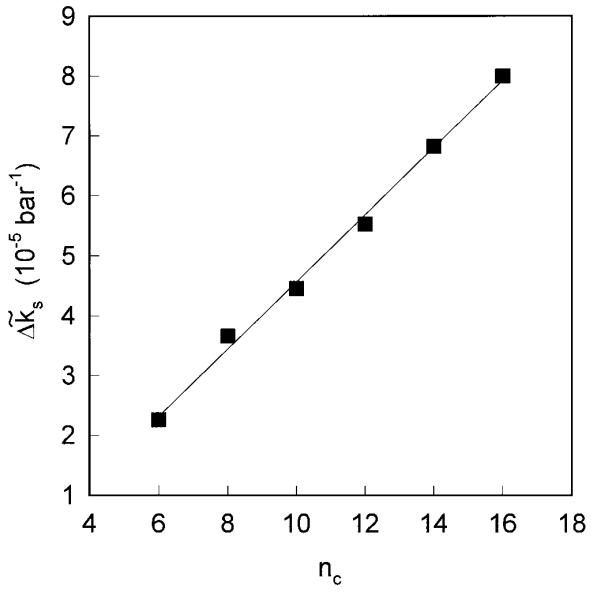

FIG. 13. Change of apparent adiabatic compressibility on micellization $\Delta\tilde{k}_S$ at 298.15 K of *n*-alkyltrimethylammonium bromides as a function of the alkyl chain length.

K. It was suggested that the low hydrophobicity of the small alkyl chain and the small size of the micelle makes the micelle more penetrable to water. Similar reasoning applied to the even smaller aggregates of C_6TAB in which there is likely to be a higher degree of exposure of the monomers within the micelle to the solvent could explain the similarity of $\tilde{k}_{S,1}$ and $\tilde{k}_{S,2}$ values.

Figure 13 shows the change of the apparent adiabatic compressibility as a result of micelle formation $\Delta\tilde{k}_S$ plotted as a function of the number of carbon atoms, where $\Delta\tilde{k}_S = \tilde{k}_{S,2} - \tilde{k}_{S,1}$. The $\Delta\tilde{k}_S$ value for C_{16}TAB was calculated from the literature (4) by linear extrapolation of data for C_nTABs with $n_c = 10$, 12, and 14. Comparison with corresponding changes of ΔS^o_m (Fig. 10) shows an increase of both with alkyl chain length. The increase of compressibility as the alkyl chain length is increased indicates a transition from an organized micellar structure at low aggregation number to a more fluid structure as the alkyl chain increases and the monomers have increased mobility.

CONCLUSION

Our investigation has shown that C_6TAB forms small aggregates (3–4 monomers per micelle) at a CMC which is lower than that predicted from the linear relationship between the CMC and the number of carbon atoms in the alkyl chain of other compounds in the homologous series of the *n*-alkyltrimethylammonium bromides. Measurements of the extent of counterion binding, the change in the thermodynamic quantities on micellization, and the apparent molar volume and adiabatic compressibilities of the aggregates have led to the proposal of a highly organized micellar structure with a large exposure of alkyl chains to the solvent.

ACKNOWLEDGMENT

The authors thank the Xunta de Galicia for financial support.

REFERENCES

1. Tanford, C., "The Hydrophobic Effect—Formation of Micelles and Biological Membranes." Wiley, New York, 1980.
2. Attwood, D., and Florence, A. T., "Surfactant Systems." Chapman & Hall, London, 1983.
3. Zielinski, R., Ikeda, S., Nomura, H., and Kato, S., *J. Colloid Interface Sci.* **119,** 398 (1987).
4. Zielinski, R., Ikeda, S., Nomura, H., and Kato, S., *J. Chem. Soc. Faraday Trans. 1* **84,** 151 (1988).
5. De Lisi, R., Ostiguy, C., Perron, G., and Desnoyers, J. E., *J. Colloid Interface Sci.* **71,** 147 (1979).
6. Jones, M. N., and Piercy, J., *J. Chem. Soc. Faraday Trans. 1* **68,** 1839 (1972).
7. Dorshow, R., Briggs, J., Bunton, C. A., and Nicoli, D. F., *J. Phys. Chem.* **86,** 2388 (1982).
8. Briggs, J., Dorshow, R., Bunton, C. A., and Nicoli, D. F., *J. Chem. Phys.* **76,** 775 (1982).
9. Drifford, M., Belloni, L., and Dubois, M., *J. Colloid Interface Sci.* **118,** 50 (1987).
10. Stigter, D., *J. Colloid Interface Sci.* **23,** 379 (1967).
11. Israelachvili, J. N., Mitchell, D. J., and Ninham, B. W., *J. Chem. Soc. Faraday Trans. 2* **72,** 1525 (1976).
12. Lee, Y. S., and Woo, K. W., *J. Colloid Interface Sci.* **169,** 34 (1995).
13. Zana, R., *J. Colloid Interface Sci.* **78,** 330 (1980).
14. del Río, J. M., Pombo, C., Prieto, G., Sarmiento, F., Mosquera, V., and Jones, M. N., *J. Chem. Thermodynamics* **26,** 879 (1994).
15. del Río, J. M., Pombo, C., Prieto, G., Mosquera, V., and Sarmiento, F., *J. Colloid Interface Sci.* **172,** 137 (1995).
16. del Río, J. M., Prieto, G., Sarmiento, F., and Mosquera, V., *Langmuir* **11,** 1511 (1995).
17. Shedlovsky, T., *J. Am. Chem. Soc.* **54,** 1411 (1932).
18. Chambers, J. F., Stokes, J. M., and Stokes, R. H., *J. Phys. Chem.* **60,** 985 (1956).
19. Pilcher, G., Jones, M. N., Espada, L., and Skinner, H. A., *J. Chem. Thermodynamics* **1,** 381 (1969).
20. Anacker, E. W., *in* "Cationic Surfactants" (E. Jungermann, Ed.), p. 217. Surfactant Science Series, Vol. 4, Marcel Dekker, New York, 1970.
21. Evans, H. C., *J. Chem. Soc.* 579 (1956).
22. Anacker, E. W., and Westwell, A. E., *J. Phys. Chem.* **68,** 3490 (1964).
23. Nusselder, J. J., and Engberts, J. B. F. N., *J. Colloid Interface Sci.* **148,** 353 (1992).
24. Phillips, J. N., *Trans. Faraday Soc.* **51,** 561 (1955).
25. Sarmiento, F., del Río, J. M., Prieto, G., Attwood, D., Jones, M. N., and Mosquera, V., *J. Phys. Chem.* **99,** 17628 (1995).
26. Conway, B. E., "Ionic Hydration in Chemistry and Biophysics." Elsevier, Amsterdam, 1981.
27. Brun, T. S., Høiland, H., and Vikingstad, E., *J. Colloid Interface Sci.* **63,** 89 (1978).
28. Tartar, H. V., *J. Colloid Sci.* **14,** 115 (1959).
29. Zana, R., Yiv, S., Strazielle, C., and Lianos, P., *J. Colloid Interface Sci.* **80,** 208 (1981).
30. Mukerjee, P., and Mysels, K. J., "Critical Micelle Concentrations of Aqueous Surfactant Systems" National Bureau of Standards NSRDS-NBS36. US Government, Printing Office, Washington, DC, 1971.

31. van Os, N. M., Haak, J. R., and Rupert, L. A. M., "Physico-Chemical Properties of Selected Anionic, Cationic and Nonionic Surfactants." Elsevier, Amsterdam, 1993.
32. Evans, D. F., Allen, M., Ninham, B. W., and Founda, A., *J. Solution Chem.* **13,** 87 (1984).
33. Evans, D. F., and Wightman, P. J., *J. Colloid Interface Sci*. **86,** 515 (1982).
34. Verral, R. E., Milioto, S., and Zana, R., *J. Phys. Chem.* **92,** 3939 (1988).
35. Muller, N., *Langmuir* **9,** 96 (1993).
36. Bashford, M. T., and Woolley, E. M., *J. Phys. Chem.* **89,** 3173 (1985).
37. Bergström, S., and Olofsson, G., *Thermochimica Acta* **109,** 155 (1986).
38. Evans, D. F., and Ninham, B. W., *J. Phys. Chem.* **87,** 5025 (1983).
39. Edsall, J. T., *in* "Proteins, Amino Acids and Peptides as Ions and Dipolar Ions" (E. J. Cohn and J. T. Edsall, Eds.), p. 157. Reinhold, New York, 1943.
40. Friedman, E., Gill, T. J., III, and Doty, P., *J. Amer. Chem. Soc*. **83,** 4050 (1961).
41. Trap, H. J. L., and Hermans, J. J., *Proc. K. Ned. Acad. Wet. Ser. B* **58,** 97 (1955).
42. Lianos, P., and Zana, R., *J. Colloid Interface Sci.* **84,** 100 (1981).